Developmental Biology 448 (2019) 237–246

Contents lists available at ScienceDirect

Developmental Biology

journal homepage: www.elsevier.com/locate/developmentalbiology

# Ci-*hox12* tail gradient precedes and participates in the control of the apoptotic-dependent tail regression during *Ciona* larva metamorphosis

G. Krasovec[a], K. Robine[a], E. Quéinnec[a], A. Karaiskou[b,1], J.P. Chambon[a,1,*]

[a] Sorbonne Université, CNRS, Institut de Biologie Paris Seine, IBPS, Evolution Paris Seine, F-75252 Paris Cedex 05, France
[b] Sorbonne Université, INSERM, Centre de Recherche Saint-Antoine (CRSA), Paris F-75012, France

ARTICLE INFO

*Keywords:*
Ascidians
Metamorphosis
Tail polarity
Tail regression
Apoptosis
*Ci-Hox-12*
Primordial germ cells
Caspases

ABSTRACT

At the onset of the *Ciona intestinalis* metamorphosis, the first event is tail regression characterized, by a contraction, an apoptotic wave and Primordial Germ Cells (PGC) movement. All these cell behaviors originate from the posterior tail tip and progress to the anterior. Interestingly, earlier in *Ciona* development, the antero-posterior (A/P) patterning of the tailbud epidermis depends on two antagonist gradients, respectively FGF/MAPK at the posterior and retinoic acid (RA) at the anterior part of the tail. Fundamental genes such as Ci-*hox1,* Ci-*hox12* and Ci-*wnt5,* classically involved in chordates A/P polarity and patterning, are controlled by these gradients and exhibit specific expression profiles in the tail epidermis. In this study, we first confirmed by video-microscopy that tail regression depends on a postero-anterior wave of a caspase-dependent apoptosis coupled with a contraction event. Concomitantly an apoptotic-dependent postero-anterior movement of PGC was observed for the first time. Unexpectedly, we observed that expression of the posterior *hox* gene, Ci-*hox12*, was extended from a posterior localization to the entire tail epidermis as the larvae progress from the swimming period to the settlement stage. In addition, when we disturbed FGF/MAPK or RA gradients we observed strong effects on Ci-*hox12* expression pattern coupled with modulation on the subsequent tail regression dynamics. These results support the idea that Ci-*hox12* expression in larval tail precedes and participates in the regulation of the postero-anterior cell behavior during the subsequent tail regression.

## 1. Introduction

The tail regression of the ascidians *Ciona intestinalis* and *Ciona robusta* represents an exciting model to investigate *in vivo* apoptosis regulation in a developmental context, since apoptosis was reported as the driving force of this process (Chambon et al., 2002), both species were used in this work but only referred as *C. intestinalis*). *Ciona* has a biphasic life cycle: a pelagic larva and a benthic adult. After fertilization, a rapid embryogenesis generates a tadpole-like larva composed of an anterior trunk and a posterior tail, consisting of approximately 2600 cells (Satoh, 1994). After hatching, the tadpole larvae swim for few hours, then adhere to a substrate and finally metamorphose into a juvenile that is a sessile filter feeder. One of the first and most dramatic events is the regression of the larval tail followed by morphological changes such as rotation of visceral organs or expansion of the branchial basket (reviewed in Karaiskou et al. (2015)).

During embryogenesis, in the elongating tail of the *Ciona* tailbud, a Retinoic Acid (RA) signaling pathway was reported, active at the anterior tail epidermis, while the FGF/MAPK and canonical Wnt pathways are restricted to the posterior tail epidermis (Pasini et al., 2012). In the *Ciona* embryo, the antagonism of these two signaling pathways is required to control the antero-posterior axis establishment and the patterning of the tail epidermis through spatial Ci-*hox1* and Ci-*hox12* expression (Pasini et al., 2012). In *Ciona*, nine *hox* genes (Ci-*hox*) have been identified: Ci-*hox1, 2, 3, 4, 5, 6, 10, 12* and *13* (Dehal et al., 2002; Spagnuolo et al., 2003). *Ci-hox1* to *5* and *Ci-hox10* and *12* seem to be involved in regionalization of the larval Central Nervous System (CNS). Moreover, at the tailbud stage (ETB, MTB, LTB), *Ci-hox12* which is expressed in the end of the posterior nerve cord and epidermis plays a pivotal role in tail development by maintaining the posterior expression of Ci-*fgf8/17/18* and Ci-*wnt5* (Ikuta et al., 2004; Ikuta et al., 2010). Inversely, *Ci-hox1* was detected at the early tailbud stage in the epidermis and the CNS around the junction of the trunk (head of the ascidian tadpole) and the tail (Ikuta et al., 2004). The FGF/MAPK signals promote Ci-*hox12* expression at the posterior-most third part of the tail while the opposite RA gradient inhibits it at the anterior-most third part and promote Ci-*hox1* expression in this region (Pasini et al., 2012). Although these expres-

* Corresponding author.
*E-mail address:* jean-philippe.chambon@upmc.fr (J.P. Chambon).
[1] The last two authors equally contributed to this work.

https://doi.org/10.1016/j.ydbio.2018.12.010
Received 31 May 2018; Received in revised form 11 December 2018; Accepted 11 December 2018
Available online 25 February 2019
0012-1606/ 

sion patterns seem to be maintained in the subsequent developmental stage, the hatching-larvae (St. 26 of Hotta et al., 2007) (Ikuta et al., 2004), data concerning Ci-*hox1* and Ci-*hox12* expression in the swimming, competent and metamorphic larvae have yet to be reported.

After the hatching stage and to reach the metamorphic changes successfully, a swimming-larva needs to acquire metamorphic competence during the larval period. This has been shown to occur in response to a wide variety of external but also endogenous signals (Jackson and Strathmann, 1981; Cloney, 1982; Davidson and Swalla, 2002; Jackson et al., 2002); review in (Karaiskou et al., 2015). In addition, we previously demonstrated that the phosphorylation of the MAP Kinases (MAPK) ERK and JNK, respectively in papillae and CNS, occurs during the competency acquisition period, and initiates a MAPK-dependent-gene-network essential for the tail regression triggering pathway (Chambon et al., 2007). When the larvae become competent, they are able to adhere to substrates with their adhesive papillae located at the anterior-most part of the trunk (Cloney, 1982; Degnan et al., 1997).

Once adhesion occurs, *Ciona* initiates tail regression. Previous studies clearly demonstrated that adhesion is a compulsory stage for this metamorphic event (Matsunobu and Sasakura, 2015; Nakayama-Ishimura et al., 2009). Indeed, when the adhesive papillae are removed ("papillae-cut" experiment), the adhesion stage is abolished and the metamorphic larvae exhibit some features of metamorphosis but never the tail regression event (Nakayama-Ishimura et al., 2009). The first tail regression mechanism proposed was based on the contractile properties of either epithelial or notochord cells that would trigger tail shortening (Cloney, 1982). More recently, we and others clearly showed that most of the tail cell types die by apoptosis (Chambon et al., 2002; Jeffery, 2002; Tarallo and Sordino, 2004). This apoptotic cell death affects the majority, if not all, of the epidermal cells of the tail, muscle cells and at least the posterior-most notochord cells (Chambon et al., 2002). The most remarkable feature of this apoptotic-dependent tail regression is its posterior origin and anterior propagation. We observed that apoptosis started at the tail tip and, through TUNEL temporal analyses, we showed that it continued up to the tail base (Chambon et al., 2002). In other words, in *Ciona*, one of the main mechanisms of tail regression is apoptosis which is tightly controlled and even predetermined in time and space along the postero-anterior axis of the larva tail; this is a unique feature among chordate organisms (reviewed in (Karaiskou et al., 2015)). Significantly, *C. robusta* genome shares with vertebrates major central actors of the cell death machinery (Takada et al., 2005; Terajima et al., 2003; Weill et al., 2005), referred as *C. intestinalis* in these publications.

As it seems to be the case in others metazoans, the achievement of apoptosis in *Ciona* occurs through the activation of cysteine proteases, termed initiator/executive caspases (Chambon et al., 2002). The vertebrate apoptotic machinery composition is substantially similar to that of non-vertebrates. In vertebrates, at least two signaling pathways are described: the "mitochondrial" (intrinsic) and the "cell death receptor" (extrinsic) pathways (reviewed in (Meier et al., 2000). In both cases, the activation of initiator caspases (8, 9 or 10) triggers a set of executioner caspases (3, 6 and 7 in mammals), strongly regulated through many layers of activators and inhibitors (Hernández-Martínez et al., 2009).

It was previously suggested that the caspases machinery diversity in *Ciona* is similar to that found in vertebrates (Baghdiguian et al., 2007). Moreover, the activation of *Ciona* caspases is essential for caudal cells elimination during tail regression (Chambon et al., 2002; Chambon et al., 2007).

Among the caudal cells, Primordial Germs Cells (PGC) are localized at the posterior part of the tail in the swimming larvae (Shirae-Kurabayashi et al., 2006). During tail regression, the PGC seem to escape from the apoptotic cell death fate. Indeed, they persist throughout tail regression with a localization described as always anterior to the regressing tail tip, suggesting a PGC movement (Shirae-Kurabayashi et al., 2006). However, no evidence was reported to associate the posterior to anterior PGC movement toward the trunk and the tail regression mechanism.

These previous observations highlight the finely orchestrated cellular events, *i.e.* contraction, apoptosis and PGC movement, in a posterior to anterior manner. However, they do not provide insights into the accurate mechanism of the sequential "destruction" of a large part of the tail tissues and the associated cellular events.

In this work, we investigated the potential role of the tail epidermis in the polarisation and coordination of these events. We first observed an extension toward the anterior of the posterior *Ci-hox12* expression. This "posteriorization" of the tail seems to be a prerequisite step for apoptosis initiation and progression. Moreover we observed that the postero-anterior PGC movement depends on the caspase-dependent apoptotic wave progression suggesting a regulation of immediate environment cell behaviors (*i.e.* PGC movement) by apoptotic cells themselves (*i.e.* wave of apoptosis), that we interpreted as an evidence of a new function of apoptosis. In addition, we were able to integrate contraction, apoptosis and PGC movement in the tail regression process.

## 2. Material and methods

### 2.1. Biological material

Adult *Ciona intestinalis* were collected on the field by the Biological Sample Collection Service of the Station Biologique de Roscoff (Britain, France) and maintained in 35‰ salinity in artificial sea water (ASW) at 18 °C in the UMR7138 Evolution Paris Seine laboratory (Sorbonne University, Paris, France). Oocytes and sperms were obtained by dissection of gonoducts and cross-fertilizations were performed in plastic Petri dishes. Embryos were cultured at 18 °C in 0.2 µm filtered ASW with 0.1 M Hepes (Sigma-Aldrich; Merck KGaA, #H4034). Tadpole larvae hatched at approximately 18 h post-fertilization (18 hpf), then, they swim freely for more than 5 h. The onset of metamorphosis started at approximately 2 h after fixation (26 hpf) when larvae adhered to plastic dishes and stop moving.

### 2.2. Fixation and storage

Larvae were fixed in 3.7% formaldehyde in phosphate-buffered saline (PBS) for 30 min at room temperature (RT) for immunofluorescent labelling. Larvae used for *in situ* hybridization are fixed 2 h at 4 °C in MEM-PFA (4% paraformaldehyde, 0.1 M MOPS pH7.4, 0.1 M NaCl, 1 mM EGTA, 2 mM MgSO4, 0.05% Tween-20). After fixation larvae are washed three times and dehydrated through a graded series of ethanol and stock in 100% ethanol at −20 °C. Rehydratation is made by successive wash series of ethanol/PBS solution to a full PBS final solution. Larvae used for TUNEL labelling were rehydrated same days of fixation and storage at 4 °C.

### 2.3. TUNEL and VASA labelling

Terminal Transferase-Mediated dUTP Nick-End labelling Assay (TUNEL) was performed with the *In Situ* Cell Death Detection Kit (Fluorescein, #11684795910) according to the manufacturer's protocol (Roche Diagnostics Corporation/ Roche Applied Science). Larvae were permeabilized in phosphate-buffered saline (PBS) + 0.2% Triton for 30 min and wash in PBS three times during 15 min. Biological samples were incubated 75 min at 37 °C in a humidification chamber with 125 µL of reaction mix (Enzyme solution plus *Label solution*). Negative control was incubated in *Label solution* only. As positive control, some larvae were incubated in DNAse I solution (1 mg/ml) (Fermentas, #EN0521) for 20 min at RT before adding the reaction mix. After reaction larvae were washed three times in PBS for 15 min.

After PBS baths larvae were incubated for the night at 4 °C in PBS + 0.1% Tween-20 (PBT) and 3% BSA (Sigma-Aldrich; Merck KGaA,

#A7906) with primary anti-Vasa antibody CiVH designed and gifted by Maki Shirae-Kurabayashi (Takamura et al., 2002; Shirae-Kurabayashi et al., 2006) and diluted at 1/500 in blocking buffer. Larvae were washed three time in PBS + 0.05% Tween-20 for 1 h, and incubated 2 h at RT in PBT + 3% BSA solution with Hoecht (1/1000) (Sigma-Aldrich; Merck KGaA, #H6024) and secondary antibody Alexa Fluor 568 goat anti-guinea pig (1/10 000) (Invitrogen, #A11075). Samples were finally washed in PBS three times for 15 min.

### 2.4. In situ hybridization

For larvae without treatment, eggs were dechorionated after insemination by immersion in ASW containing 1% sodium thioglycolate (Sigma-Aldrich; Merck KGaA, #T0632) and 0.05% Pronase E (Sigma-Aldrich; Merck KGaA, #P5147). Then, the eggs were washed (washing must be done before first division) and placed in 1.5% low gelling agar-coated (Sigma-Aldrich; Merck KGaA, #A9414) Petri dishes in ASW 0.5% bovin serum albumin (BSA) (Sigma-Aldrich; Merck KGaA, #A7906).

For the larvae used to perform *in situ* hybridization of Ci-*hox12* in treatment conditions, we decide to remove the tunic manually. Tunic was removed from the entire tail and not the trunk because of the risk to cleave the larvae in two parts. Huge larvae samples must be dissected to obtain a final number of 10 and 20 larvae available because of the very delicate procedure. This procedure allows us to obtain ISH whole-mount larvae without strong background generated by the tunic and an accurate labelling interpretable without doubt. Indeed tunic is a strong problem when working with larvae after hatching in opposite with developing larvae.

Larvae were fixed 2 h at 4 °C in MEM-PFA (4% paraformaldehyde, 0.1 M MOPS pH7.4, 0.1 M NaCl, 1 mM EGTA, and 2 mM MgSO4, 0.05% Tween-20). After fixation larvae were washed three times and dehydrated through a graded series of ethanol/PBS baths and stocked in 100% ethanol at −20 °C. Rehydratation was made by successive washes of ethanol/PBS solution to a full PBS final solution. Hybridization was made according to the protocol of (Christiaen et al., 2009) except that methanol was replaced by ethanol. Probes were tested on LTB to control that the labelling was in accordance with pattern data from ANISEED before larva processing.

### 2.5. Pharmacological treatments

Swimming larvae were distributed in small Petri dishes after hatching. If number of larvae allows it, three biological replicates were made for each treatment. When 70% of larvae were settled on the dish and when some of them were not moving anymore - this mean that metamorphosis will begin soon - supernatant was discarded and replaced by filtered ASW containing each pharmacological treatments or dimethylsulfoxid (DMSO) (Sigma-Aldrich; Merck KGaA, #D8418) as control. Drugs were stored in DMSO at −20 °C. Pan-caspases inhibitor benzyloxycarbonyl-Val-Ala-Asp-fluoromethyl ketone (Z-VAD-FMK) (Sigma-Aldrich; Merck KGaA, #V116) was used at final concentration in ASW at 10 μM SU5402 (Sigma-Aldrich; Merck KGaA, #SML0443), retinoic acid (RA) (Sigma-Aldrich; Merck KGaA, #R2526) and diethylaminobenzaldehyde (DEAB) (Sigma, #D86256) were used at final concentration of 1.5 μM, 10 μM, and 150 μM respectively. U0126 (Promega, V1121) and SP600125 (Sigma-Aldrich; Merck KGaA, #S5567) were used at final concentration of 6 μM and 10 μM respectively. For each treatment, same quantity of DMSO was added in all controls.

### 2.6. Measures and statistics

The beginning of the tail regression in the control allows determining the T0 of the experiments. From this starting point, proportions of larvae with tail regression in progress were calculated at different time (2, 4 and 6 h) in each treatment. PGC relative position was evaluated by calculated the ratio (Z) between the posterior length behind the PGC (PL) and the anterior length in front of the PGC (AL). Differences between all conditions take together (DMSO, DEAB, RA, SU) were evaluated by Kruskal-Wallis analysis. Differences between control and each condition taken separately were made by Wilcoxon Mann Whitney test. Effects were considered significant with a p-value < 0.05. All statistics were done using tools implemented in the stats package of the software R 2.14.1 from the R Development Core Team (2011) (R: A language and environment for statistical computing. Vienna, Austria: R Foundation for Statistical Computing. Available: www.R-project.org).

### 2.7. Microscopy and Image acquisition

Images are taken with a confocal Leica TCS SP5 microscope and an Olympus BX61 microscope. All images are analysis with ImageJ 1.46a-1 software version or the LAS AF Lite. Images with DAPI labelling were treated by ImageJ filters to well delimit the nuclei contour (Process-Filters-Convolver). Larvae pictured in several parts was reconstruct with ImageJ Fiji (Plugins-Stitching-Pairewise stitching) Macroscopes used for the *in vivo* video is a whole *Ciona* larvae were mounted on glass slides and coverslipped with Mowiol 4–88 (Calbiochem, #475904). Images were acquired with a BX61 microscope (Olympus) and a confocal TCS SP5 microscope (Leica). Sequential optic sections were acquired in z-stacks and processed using ImageJ 1.46a-1 software version or the LAS AF Lite.

### 2.8. In vivo macroscopy

Settled larvae were harvest and bathed in ASW contained the live fluorescent marker of caspase activity Cell Event Caspase-3/7 Green Detection Reagent (Invitrogen, #C10423) for a final concentration of 20 μM during 2 h. They were anesthetized in ASW containing 200 mg/L of ethyl-3-aminobenzoate methylsulfonate (MS222)(Sigma-Aldrich; Merck KGaA, #E10521**)** and then immobilized in ASW containing 0.25% agarose low melting (Sigma-Aldrich; Merck KGaA, #A9414) in Ibidi μ-Slide VI 0.1 (Biovalley, #80661). Temperature is maintained at 18 °C. Images were taken with a Macro-Apotome (ZEISS).

### 2.9. Papilla cut experiments

Papilla cut was realized according to the protocol of Nakayama-Ishimura et al. (Nakayama-Ishimura et al., 2009).

## 3. Results

### 3.1. Polarized Caspases activation, apoptosis onset and PGCs movement are major postero-anterior events during tail regression

Among the executive caspases, we previously reported that a Caspase 3-like protein is expressed and activated during *Ciona* metamorphosis (Chambon et al., 2002). In order to follow *in vivo* activation of this executive caspase (Ci-Caspase 3-like) in *Ciona intestinalis,* prior to tail regression, we combined time-lapse microscopy and activated caspases-labelling using a fluorescent marker (“caspase event 3/7”) (video 1 and video 2). For this approach, we embedded live larvae in low gelling agarose in order to limit tail movement during the time-lapse acquisition. Using this experimental approach, we were able to detect, at the onset of the metamorphosis a discrete shortening (about 10% of total length) that occurs at the posterior tail tip just before caspases’ activation (video 1 and 2). This process is followed by a wave of fluorescent labelling which progresses along the tail from the posterior tip to the trunk. This event corresponds to executive caspases activation starting at the tail extremity and propagating towards the tail basis.

Supplementary material related to this article can be found online at doi:10.1016/j.ydbio.2018.12.010.

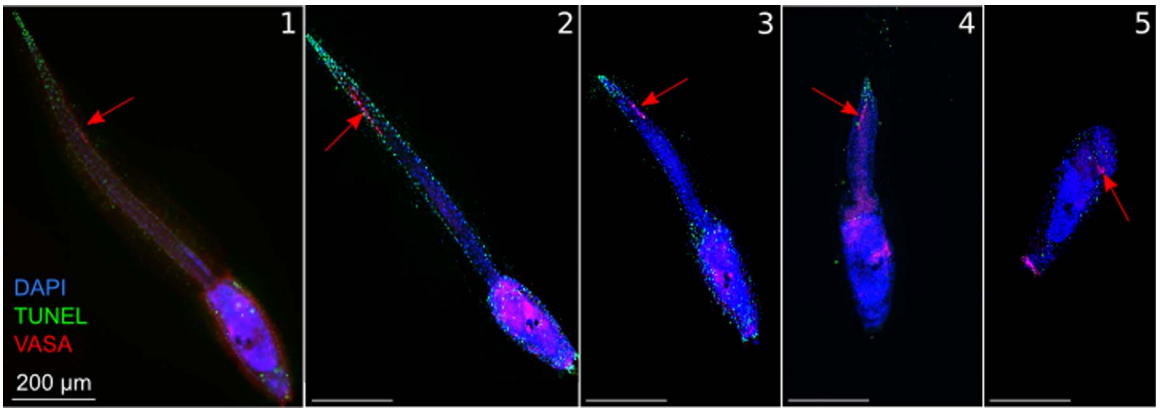


**Fig. 1.** PGCs move simultaneously with the apoptotic wave propagation during *Ciona* tail regression. Double VASA (red) and TUNEL (green) labelling was performed with DAPI (blue) in settled larvae during tail regression. During the temporal sequence of tail regression, TUNEL positive cells are localized posteriorly of the PGCs and synchronously move towards the trunk. The apparent modification of the PGC row organization is essentially due to different orientation of the larvae at the time of the picture acquisition and may not reflect the *in vivo* exact position with an exception for the last picture. Indeed we often observed this apparent grouping of PGC at the end of tail regression. To evaluate the relative position of the PGCs, we have calculated the ratio (Z) between the posterior length behind the PGC (PL) on the anterior length in front of the PGC (AL). The Z indice, is respectively for image 1: Z = 0.4490, image 2: Z = 0.3803, image 3: Z = 0.3595 and image 4 Z = 0.3667. We precise that the Z indice calculated here are in accordance with the data range shown in Fig. 4D. (For interpretation of the references to color in this figure, the reader is referred to the web version of this article).

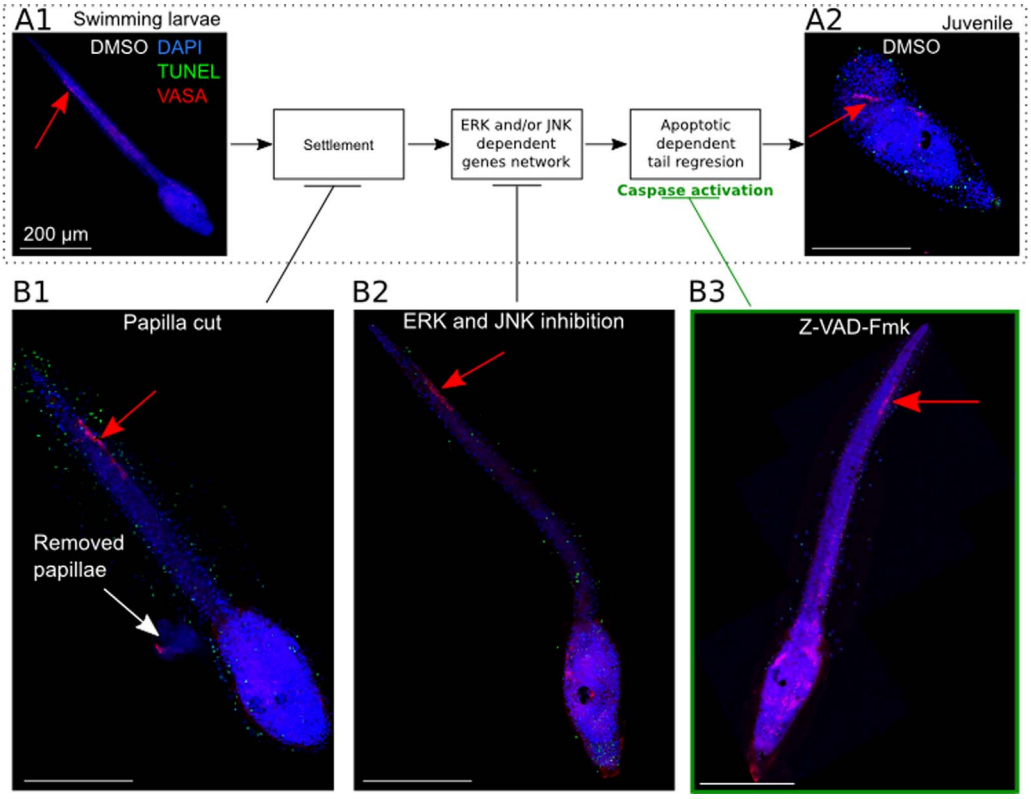


**Fig. 2.** PGC movement is a part of the tail regression and is controlled by apoptosis. Double VASA (red) and TUNEL (green) labelling was performed with DAPI (blue) in four conditions, respectively in B1 (papillae cut – no adhesion), B2 (treated with 6uM U0126 – MAPK kinase inhibitor; or 10 µM SP600125 – JNK inhibition, in ASW) and B3 (treated with 10 µM Z-VAD-Fmk – pan-caspases inhibitor in ASW). (A) Control situation: After fixation swimming larvae activate the ERK and JNK dependent genes network, the apoptotic tail regression occurs, and finally larvae lose their tail but PGC are present in the trunk. (B) Inhibition of the apoptotic wave by three independent approaches, blocks tail regression and PGC movement. Because of papillae removal, adhesion is impossible and the first step of metamorphosis does not occur for none of the larvae (116/116) (B1). ERK and JNK inhibition blocks the gene network leading to the tail regression initiation of 84,9% (980/1154) and 91,9% (1106/1204) of larvae respectively (B2). Caspases activity inhibition by Z-VAD-Fmk, inhibits tail regression of 76,6% of the larvae (1056/1377) (B3). (For interpretation of the references to color in this figure legend, the reader is referred to the web version of this article).

Given the physical constraint imposed to the larvae in this approach (see materials and methods for details) due to low gelling agarose, we assumed that we slowed down the tail regression process (each video corresponds to 4 h acquisition). We always observed the same specific time sequence of events, and the co-existence of two distinct temporal phenomena: a physical contraction followed by a caspase activation. Moreover, this time lapse approach confirms that both, contraction and apoptosis start at the most posterior part of the tail, with apoptosis extending to the anterior part and seemingly affecting the vast majority of the caudal cells.

PGC labelling using a polyclonal anti-Vasa antibody (a well-known PGC marker) coupled with a TUNEL staining, confirms that PGC movement co-occurs with tail regression in *Ciona intestinalis* (Fig. 1), as in *Ciona robusta* (Shirae-Kurabayashi et al., 2006). However, as shown in Fig. 1 (red arrow), Vasa labelling precedes the TUNEL staining and co-localization between TUNEL and Vasa was not

observed. This result implies that PGC move towards the trunk while being just at the anterior front of the apoptotic wave meaning that the relative position of PGC (Fig. 1, Z indice) is maintained just anterior to the apoptosis wave during the full process. Taken together these results suggest that all three processes (contraction, apoptosis and PGC movement) are coordinated during tail regression in a posterior to anterior manner and we focused on the last two for the rest of the study.

### 3.2. PGC movement is coordinated with the cellular events of the tail regression

The PGC movement described above could be either independent but concomitant to the apoptotic regression wave or participate in a coordinated process.

The onset of metamorphosis comes after the acquisition of competence and is correlated with the definitive adhesion of the larvae to the substratum (Matsunobu and Sasakura, 2015; Nakayama-Ishimura

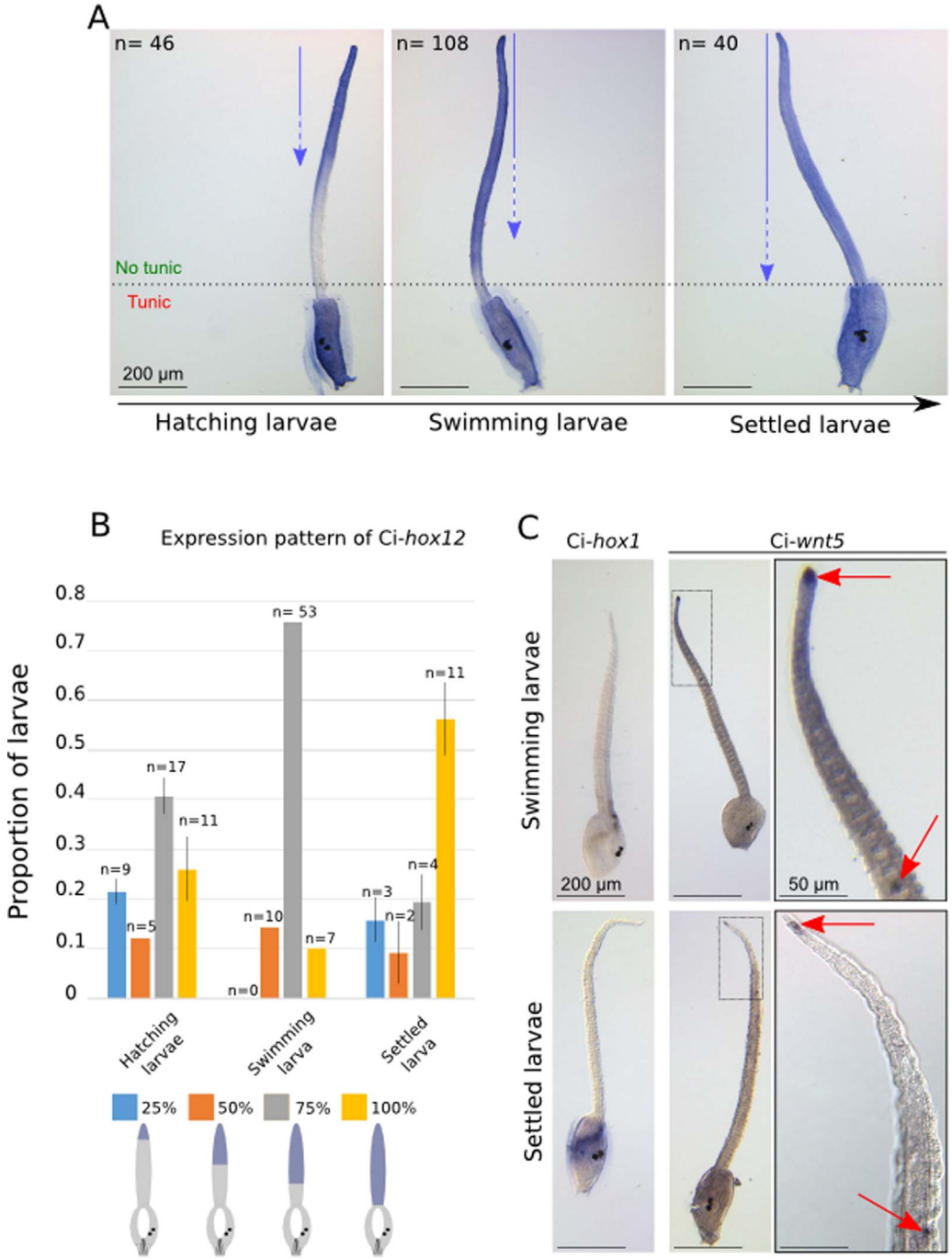


**Fig. 3.** *Ci-hox12* expression is extended to all the tail prior to the tail regression. *In situ* hybridization of Ci-*hox12* (KH2012: KH.C7.472) on larvae at different times: hatching larvae; swimming larvae and settled larvae; *In situ* hybridization on swimming larvae and settled larvae (pre-metamorphic) of Ci-*hox1* (KH2012: KH.L171.16) and Ci-*wnt5* (KH2012: KH.L152.45). (A) Ci-*hox12* is expressed at the posterior part of the tail. Before tail regression initiation, expression propagates throughout the tail and finally to the whole tail. (B) Quantification in percentage of the surface of labelling (from the tip toward the base) observed in the tail for each time of observation (*i.e.* hatching, swimming and settled larvae). Standard deviation is indicated if enough biological replicates were available to calculate it. (C) *Ci-hox1* and *Ci-wnt5* expression pattern in larva resembles the embryo pattern. Ci-*hox1* is expressed at the same localization at both stages, at the visceral ganglion and the endoderm in the trunk. Ci-*wnt5* is expressed at the same localization at both stages, at the posterior extremity of the tail, and at some cells localized ventrally in the endodermal strand (red arrows).

et al., 2009). Adhesion is followed by ERK and JNK-dependent-genes-network activation that controls apoptosis initiation at the tip of the tail (Chambon et al., 2007). To abolish each of these initiating steps we either prevented adhesion of the larva by the well-described "papillae cut" experiment (Nakayama-Ishimura et al., 2009) or by ERK or JNK inhibition (using their respective selective inhibitors, U0126 and SP600125) that block the subsequent genes network onset and subsequently tail regression (Chambon et al., 2007) (Fig. 2). We combined a double Vasa/TUNEL labelling to these treatments to analyse PGC localization at a time when PGC reach the trunk in the DMSO control larvae (Fig. 2 . A2). In both experiments (Fig. 2. B1-B2) we observed that the onset of the tail regression has been abolished as expected and that the PGC are still localized at the posterior of the tail similarly to the swimming larvae, meaning that the PGC movement depends on the onset of the tail regression event. Our results suggest that the apoptotic wave and the PGC movement depend on the same initial molecular cue switching on the tail regression but they do not inform us on their interdependence. In order to investigate this process, we used a pan-caspase inhibitor (Z-VAD-Fmk) that abolishes apoptotic dependent tail regression by blocking caspases activation (Chambon et al., 2002) (Fig. 2. B3). Once again, the onset of the tail regression has been abolished as apoptosis has been inhibited and in a more interesting way the PGC were still localized at the posterior part of the tail as in the swimming larvae, meaning that the PGC movement depends on the apoptotic events.

These results highlight that PGC movement is a cellular mechanism that belongs to the metamorphic sequence, and should be coordinated with other postero-anterior cellular behaviors such as apoptosis. Moreover, the chemical inhibition of caspases blocks PGC movement supporting the fact that PGC movement depends on apoptosis progression.

### 3.3. Ci-*hox12* expression is extended in all the tail prior metamorphosis

It has been reported that in the *Ciona* embryo, antero-posterior polarity of the tail epidermis depends on the antagonism of the RA and FGF/MAPK (Pasini et al., 2012). Furthermore, Ci-*hox12* role has been established into maintaining the posterior expression of Ci-*fgf8* and Ci-*wnt5* and it has been proven essential for the tail tip formation (Pasini et al., 2012; Ikuta et al., 2010). We hypothesized that these early events could be linked to polarized mechanisms of the tail regression (*i.e.* apoptotic wave, PGCs movement) but also to other molecular cues (see Fig. 2). We investigated the expression profiles of these genes involved in tail epidermis patterning in *Ciona* (Ci-*wnt5*, Ci-*hox1, and* Ci-*hox12)* from the hatching larva to the settlement stage (Fig. 3).

No difference was observed for Ci-*wnt5* between swimming and settled stage where it is expressed at the tip of the tail and in some ventral cells (red arrows, Fig. 3C) and as reported in previous studies (Pasini et al., 2012). Ci-*hox1* is expressed at the anterior part of the tail, the dorsal trunk border (*i.e.* probably the visceral ganglia as reporter in (Ikuta et al., 2004)) and at the posterior part of the trunk in swimming larva and seems to be restricted and extended in the trunk in settled larva (Fig. 3C). These observations are in accordance with previous observations (Pasini et al., 2012; Ikuta et al., 2004).

A contrasted situation was observed for Ci-*hox12* expression between swimming and settled larvae (Fig. 3A). Previously, Ci-*hox12* expression was reported in the very posterior part of the tail during embryogenesis, at the mid-tailbud and late-tailbud stage (Pasini et al., 2012). In swimming larva, Ci-*hox12* expression is extended to the posterior half of the tail (Fig. 3. A), and is present throughout the tail at the fixation stage (Fig. 3. B, the strong background in the trunk observed at this stage is due to a thick larval tunic, often producing high unspecific signal observed in this region). Given this, Ci-*hox12* gene expression evolving from the posterior tail towards anterior, is compatible with the role of potential molecular cue driving postero-anterior caspase-dependent-apoptosis and PGC movement.

### 3.4. Ci-*hox12* expression modulation disrupts the apoptotic wave and the associated PGCs movement

In order to test this potential role of Ci-*hox12*, we modulated its expression. We therefore treated settled larvae with either RA, DEAB (inhibitor of RA synthesis) or SU (inhibitor of the FGF pathway) and followed Ci-*hox12* expression (Fig. 4. A).

As it was reported previously, RA and SU treatment strongly affected Ci-*hox12* expression (Pasini et al., 2012). In settled treated larvae we were not able to detect Ci-*hox12* expression in the tail by *in situ* hybridization (Fig. 4. A, lower panel). On the contrary when we treated settled larvae with DEAB, we observed a stronger expression in all the tail in comparison with the DMSO control (Fig. 4. A, upper panel). The strong background observed at this stage, due to a thick larval tunic obliged us to manually remove the tunic from the larva tail prior to *in situ* hybridization.

We took advantage of this Ci-*hox12* expression modulation to observe the effect on tail regression speed (Fig. 4. B). We compared percentage of larvae with tail regression in progress at different time points between all treatments and notice differences between them (Kruskal-Wallis chi-squared = 47.1334, df = 3, p-value = 1.43e-09). The same observation was made between the control and each treatment. We clearly observed that tail regression occurs faster with DEAB (W = 365, p-value = 1.312e-06) treatment compared with the control (DMSO), and an opposite situation occurred with RA (W = 102.5, p-value = 0.0001272) and SU (W = 78.5, p-value = 0.02101) treatment in which the process is delayed at all times. This result strongly correlates tail Ci-*hox12* expression with the subsequent tail regression process during metamorphosis.

We next analysed apoptosis in treated larva (with DEAB, RA or SU), at the time where apoptosis should be initiated at the tip of the tail in control (DMSO). Interestingly, apoptosis already started to propagate as a wave in DEAB-treated larva while apoptosis was not initiated in SU- and RA-treated larva (Fig. 4. C). Since apoptosis was reported as the driving force of the tail regression, this result confirms the previous result on the positive effect of Ci-*hox12* expression on apoptotic-dependent tail regression in *Ciona*.

Finally, we measured the relative position of the PGC during the tail regression at different time (Fig. 4. D1-D2) and found no differences between all treatments (Kruskal-Wallis chi-squared = 1.5787, df = 3, p-value = 0.6642). We found equivalent results when we compared each treatment with the control (DMSO), respectively DEAB (W = 2127, p-value = 0.5243), RA (W = 1468, p-value = 0.8656) and SU (W = 453, p-value = 0.2939). It clearly appeared that PGC move towards the trunk in accordance with the progression of apoptosis and the associated tail regression. In other words, when apoptosis propagated faster, the PGC reached the trunk faster, and on the opposite when apoptosis propagated slower, the PGC moved slower. Moreover, we combined DEAB with pan-caspase inhibitor (Z-VAD-Fmk) treatment (Supplemental Fig. A, B) and we confirmed that PGC movement is effected by the caspase dependent-apoptotic wave and not a parallel effect of the DEAB.

Taken together these results offer an obvious link between the dynamic expression pattern of Ci-*hox12* in the larva tail and the subsequent tail regression during metamorphosis. Moreover, Ci-*hox12* participates in the initiation and the dynamics of the tail regression by influencing the cell behaviors involved in this process such as apoptosis and the subsequent PGC movement. These data demonstrated that the extension of Ci-*hox12* from the posterior part to anterior part of the tail in the swimming and settled larvae is an excellent compulsory cue candidate for *Ciona* tail regression.

## 4. Discussion

This study focuses on the cellular and molecular mechanisms that drive the tail regression during *Ciona* metamorphosis.

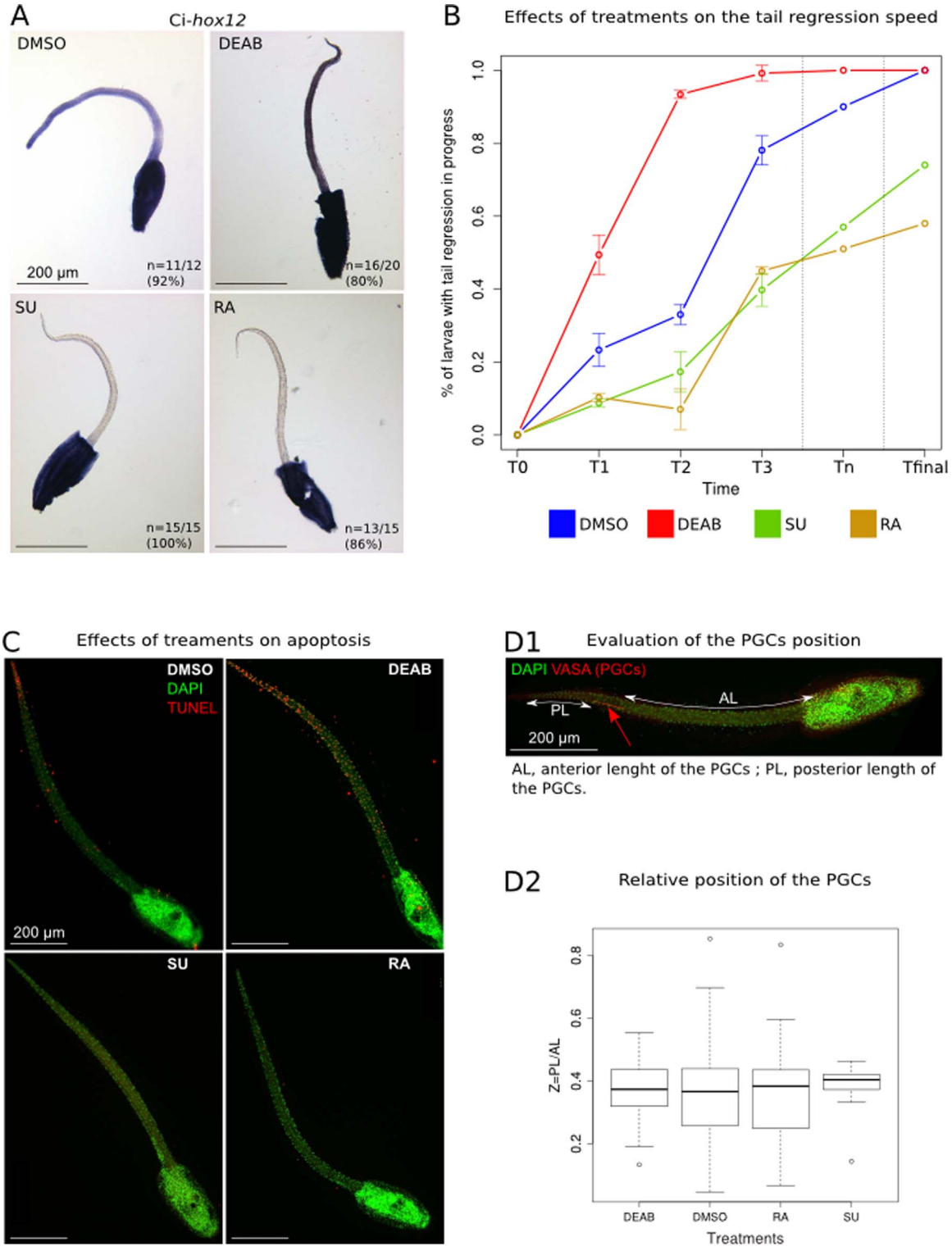


**Fig. 4.** Modulation of *Ci-hox12* expression affects tail shortening events : propagation of apoptosis and PGC movement. (A) In situ hybridization of Ci-*hox12* expression in the pre-metamorphic larvae tail after DMSO (control), DEAB (RA inhibitor, 150 µM), RA or SU (FGF inhibitors, used at 10 and 1, 5 µM respectively) treatments. The expression gradient is present in control and in DEAB treated larvae (where the labelling is even stronger) in contrast with RA and SU where no labelling is observed. Total absence of tunic on the trunk made the observation of the signal more obvious. (B) Percentage of larvae with tail regression in progress for the different treatments. The frequency is calculated over time for each condition. By statistical tests (Kruskall-Wallis test), we show that proportion of larvae with tail regression in progress is statistically different between all conditions. Same differences are shown (Wilcoxon Mann Whitney test) between control and each treatment taken separately. More than 6000 larvae from 23 independent fertilizations were used. (C) TUNEL labelling (red) with DAPI (green) in larvae treated with DEAB, SU or RA (concentrations as mentioned above) at the time of initiation of apoptosis in control (as in DMSO). As expected, more TUNEL positive cells are present in DEAB conditions in opposite with RA and SU where not TUNEL positive cells are present. (D) To evaluate the relative position of the PGCs, we have calculated the ratio (Z) between the posterior length behind the PGC (PL) on the anterior length in front of the PGC (AL). The ratio is calculated for each treatment on larvae with tail regression in progress, allowing us to obtain the PGCs relative position and an estimation of their movement speed. Differences between all conditions (Kruskall Wallis test), and between the control and each treatment (Wilcoxon Mann Whitney test) are not significant. There is no effect of the drugs, involving that the PGCs move at same speed as the tail regression. These calculations were performed on 207 larvae from 5 independent fertilizations.

### 4.1. Contraction and apoptosis act together during tail regression

We previously reported that apoptotic cell death could be considered as the driving force of the tail regression during metamorphosis (Chambon et al., 2002; Chambon et al., 2007), since when apoptosis is abolished, *i.e.* with pan-caspase inhibitors, the tail regression is inhibited (Chambon et al., 2002) and this study). However, here we observed a first step of contraction (video 1 and 2), that concerns the tip of the tail, and which precedes caspase activation and results in a shortening process. It would be interesting to address if this contraction is a prerequisite to the initiation of apoptosis in this same region.

Another noteworthy observation from our videomicroscopy approach is that the tail continues the shortening process during the progression of both the PGCs and the apoptosis wave towards the trunk (Fig. 1). It will be challenging to figure out how this process occurs in an apoptotic context (video 1 and 2). Indeed, executive caspases activation is well known to highly disorganize the actin cytoskeleton and global cellular organization (reviewed in Vaculova and Zhivotovsky (2008)), which is not compatible with contractile events, as the one suggested by Cloney (1982) proposing that the epidermal layer moves and pushes the other tissues toward the trunk during tail regression. Another puzzling fact is that we never observed any cell corpse clearance (apoptotic bodies phagocytosis) of the dead cells during tail regression, which is considered as the ultimate event of this physiological cell death. In *Caenorhabditis elegans*, *Drosophila melanogaster* and in vertebrates the engulfment step leads to the recycling of the dead cells energy (reviewed in (Klöditz et al., 2017)). In *Ciona*, the shortening process could provide an excellent way to bring the dead cells toward the trunk and it would be tempting to hypothesize that the dead cells are engulfed by trunk cells in order to provide energy for the subsequent events of the metamorphosis.

### 4.2. Ci-hox12 is involved in the apoptosis regulation during tail regression

In the present study, we show that Ci-*hox12* expression is extended to all the tail just before the tail regression onset (Fig. 3). Moreover this extension is required for the tail regression and manages the apoptosis progression and the associated PGC movement (Fig. 4., Figs. 4,5). Hox-regulated apoptosis was already reported in metazoans (review in (Domsch et al., 2015)). In vertebrates, during the limb development, interdigital cell death is indirectly regulated by *Hox*A13 (Knosp et al., 2004). In *Drosophila*, the transcriptional activation of the pro-apoptotic protein Rpr by the anterior *Hox* gene *dfd* is required for the formation of the maxillary/mandibular segment boundary (Lohmann et al., 2002). Moreover, the posterior *Hox* gene *abd-A* activates pro-apoptotic genes in drosophila neuroblasts that die by apoptosis, in a cell autonomous manner (Bello et al., 2003). This work also suggests a regulation of apoptosis by *Hox* genes at a specific developmental timing. An interesting mechanism would be a transcriptional control of pro-apoptotic proteins at the same time we observed Ci-*hox12* expression extended throughout the tail. Interestingly, Ci-*caspase 3* is expressed during the swimming period in the larva and activated during *Ciona* metamorphosis, but is undetectable at the hatching stage (Chambon et al., 2002).

However, the major function of *Hox* genes is the patterning of the A-P axis during metazoan embryogenesis (Hueber and Lohmann, 2008). In vertebrates, *Hox* genes establish the pattern of the central nervous system and vertebrae along the A-P axis (Altmann and Brivanlou, 2001; Koussoulakos, 2004; Mallo et al., 2010). In *Ciona*, a limited role for 3 out of 9 *Hox* genes was reported during larval development, Ci-*hox1* is required for anterior gut formation *via* regulation of larval, atrial siphon primordium formation (Sasakura et al., 2002); Ci-*hox10* is involved during development of GABAergic neurons in the dorsal visceral ganglion and Ci-*hox12* play important roles in tail development and morphology (Ikuta et al., 2010). Interestingly, Ci-*hox10* is also required later to promote migration of endodermal strand in swimming larvae (Kawai et al., 2015). This process is regulated indirectly by Ci-*hox10* by reconstructing the extracellular matrix through direct regulation of the expression of the collagen type IX (Kawai et al., 2015). In other words, Ci-*hox10* promotes endodermal strand cells survival by indirectly regulating their migration. In our case, we could hypothesize that Ci-*hox12* promotes PGC survival by indirectly regulating their movement through apoptosis regulation.

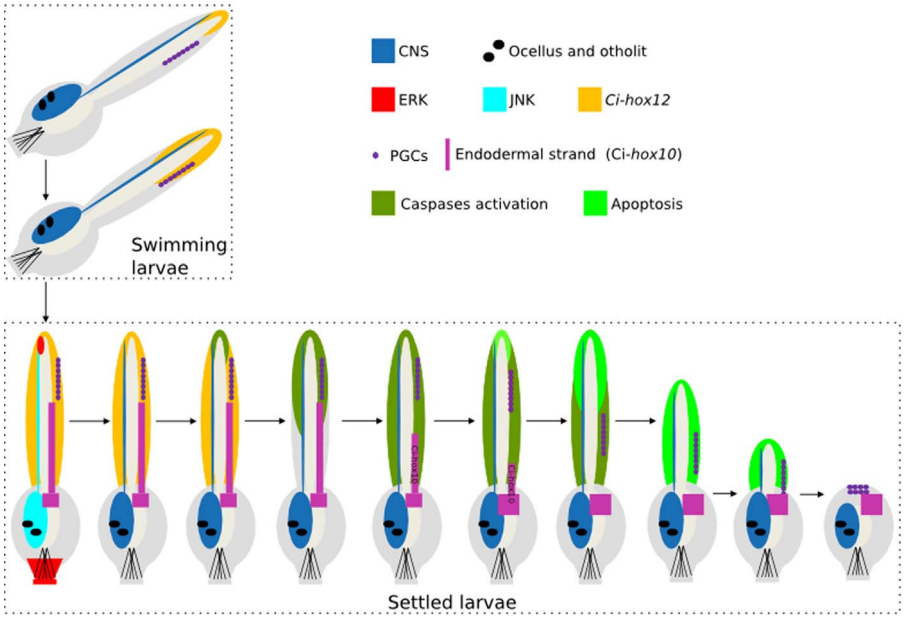


**Fig. 5.** Schematic representation of the temporal sequence of polarized events that happen during the tail regression. During the swimming period, the Ci-*hox*12 expression extends from the posterior part of the tail to the trunk. In settled larvae, caspases activation wave starts at the tip of the tail and propagates as a wave to the anterior part. Consequently an apoptotic polarized wave occurs and triggers the tail regression. Caspase-dependent apoptosis promotes the PGC migration which moves at the same time to reach the trunk (Black arrow). In *C. intestinalis* the question of endodermal migration promoted by apoptotic cells is still open (black arrow dash-line).

### 4.3. Apoptosis manages PGC movement in a caspase-dependent manner

During tail regression, one of the emerging issues of our investigation is the compelling fact that groups of cells in the will survive, as it is the case of the endodermal strand and the Primordial Germ Cells (PGC) ((Shirae-Kurabayashi et al., 2006; Kawai et al., 2015), this study). Furthermore, these two latter groups of cells achieve survival, at least partially, by a posterior to anterior migration, which takes place in swimming larva (Kawai et al., 2015) or at the onset of tail regression (our unpublished observation) for the endodermal strand, or during tail regression for the PGC (Fig. 1). For the later ones, apoptotic cells in ascidians tail could act as a driving force for their migration towards the trunk. Indeed, when apoptosis is inhibited with a pan-caspase inhibitor, PGC stay in the posterior part of the tail (Fig. 2. B3), which implies that caspases activity is necessary for this movement. Moreover, taking advantage of the polarisation of this event, we successfully modulated the dynamics, *i.e.* the speed, of the apoptotic wave using chemical treatments that perturb tail polarity (Fig. 4). We observed that the speed of PGC migration positively correlates with the speed of the apoptotic wave toward the trunk (Fig. 4C, D). Taken together these results strongly suggest an apoptosis-dependent-PGC movement toward the trunk. Apoptosis-dependent cell migration was already reported in several vertebrate systems. During mouse development, it was suggested that migration of olfactory sensory neuron is mediated by caspase activity. In these cells the cleavage of a membrane-anchored member of the semaphorin family of guidance proteins, Sema7A, is correlated to Caspase 3 activation. Caspase 3 KO or its upstream regulators Apaf-1 or Caspase 9 affect axonal path finding, synapse formation and maturation status in the olfactory bulb (Ohsawa et al., 2010). During tail regeneration in Xenopus laevis tadpole, when apoptosis is abolished, a mis-patterning of axons is observed, suggesting an apoptotic dependent axon guidance mechanism (Tseng et al., 2007). It is tempting to hypothesize that apoptotic cells in the regressing *Ciona* tail may provide molecular cues that activate PGC movement.

Studies on metamorphosis in insects and amphibians, where some larval structures are eliminated by apoptosis (Tata, 1966; Lockshin and Williams, 1965) and the work on embryogenesis in some Bilateria, where apoptosis sculpts developing structures by elimination of supernumerary cells, led to the definition of the “sculpting model” or “carving model”. Apoptosis is a genetically controlled programmed cell death mechanism, considered crucial for metazoan development because of its function in cell removal, described for example during digit formation in tetrapods vertebrates (Hernández-Martínez et al., 2009); review in Suzanne and Steller (2013). During the last decades, research from different systems increased evidence on apoptotic-dependent cell behaviors and tissue remodeling during morphogenesis, in addition to the destructive function. It was reported that caspase-dependent signals of dying cells towards their vicinity participate in morphogenetic processes. This signaling can be mediated by: (i) exerting mechanical forces inside the tissues that participate actively to tissue (re) modeling (Monier et al., 2015; Toyama et al., 2008; Yamaguchi and Miura, 2013); (ii) caspase-dependent secreting molecular cues that affect the behaviors of the surrounding cells inducing cell proliferation (Vritz et al., 2014; Chera et al., 2009; Chera et al., 2011; Huh et al., 2004; Tseng et al., 2007; Li et al., 2010), cell differentiation (Seipp et al., 2001), cell migration (Ohsawa et al., 2010; Tseng et al., 2007; Lauber et al., 2003; Gude et al., 2008), or promoting cell survival (Bilak et al., 2014).

Tail regression of *Ciona* represents an excellent model to address the molecular relationship between apoptotic cells and PGC movement.

## 5. Conclusion

The results of this work taken with previous observations on ascidian metamorphosis (reviewed in Karaiskou et al. (2015) lead us to propose a model (Fig. 5) in which the extension towards the anterior part of the tail of Ci-*hox12* expression is the first molecular event in the tail prior to the tail regression process. It will be now interesting to address the temporal coordination and the potential link between the molecular and cellular events from the swimming period to the apoptotic wave and the PGC movement. However, it is also crucial to distinguish common from specific mechanisms between the two *Ciona* species, *i.e.* C. *intestinalis* and *C. robusta*. Indeed, we have already identified some interesting differences in the time sequence of events. For example Ci-*hox10*-dependent endodermal strand migration was reported during the swimming period in *C. robusta* (Kawai et al., 2015), while we observed this migration process at the onset of tail regression (unpublished data) in *C. intestinalis*. The comparison of the time sequence of metamorphic events between these two phylogenetically close species should provide clues on the evolution of the metamorphic process.

## Acknowledgements

We acknowledge Dr Shirae-Kurabayashi for the kindly gift of the Ci-Vasa antibody; J.F. Gilles (plateforme imagerie, IBPS/Sorbonne Université) for assistance in time-lapse acquisition with Zeiss macro-apoptome. We also acknowledge the “André Picard” network community, S. Darras and A. Roure (Observatoire océanologique de Banyuls sur Mer/Sorbonne Université), C. Vesque (IBPS/Sorbonne université) and J. Gros (Institut Pasteur, Paris) for helpful discussion; the IBPS animal facility.

## Funding

The work of G.K. was supported by a Ph.D. fellowship from the French Ministry of Education, research and Innovation, by “André Picard” fellowship "Projet collaboratif exploratoire".

The present study was supported by Foundation ARC pour la recherchesur le cancer grant n°PJA 20141201892 to JP. Chambon and “Emergence recherche sur UPMC” grant attributed to JP. Chambon and A. Karaiskou.

## Appendix A. Supporting information

Supplementary data associated with this article can be found in the online version at doi:10.1016/j.ydbio.2018.12.010.

## References

Altmann, C.R., Brivanlou, A.H., 2001. Neural patterning in the vertebrate embryo. Int. Rev. Cytol. 203, 447–482.
Baghdiguian, S., Martinand-Mari, C., Mangeat, P., 2007. Using *Ciona* to study developmental programmed cell death. Semin. Cancer Biol. 17, 147–153.
Bello, B.C., Hirth, F., Gould, A.P., 2003. A pulse of the *Drosophila* Hox protein Abdominal-A schedules the end of neural proliferation via neuroblast apoptosis. Neuron 37 (2), 209–219.
Bilak, A., Uyetake, L., Su, T.T., 2014. Dying cells protect survivors from radiation-induced cell death in *Drosophila*. PLoS Genet. 10 (3), e100422, (Mar 27).
Chambon, J.P., Nakayama, A., Takamura, K., McDougall, A., Satoh, N., 2007. ERK- and JNK-signalling regulate gene networks that stimulate metamorphosis and apoptosis in tail tissue of ascidian tadpoles. Development 134, 1203–1219.
Chambon, J.P., Soule, J., Pomies, P., Fort, P., Sahuquet, A., Alexandre, D., Mangeat, P.H., Baghdiguian, S., 2002. Tail regression in *Ciona intestinalis* (Protochordate) involved a Caspase-dependent apoptosis event associated with ERK activation. Development 129, 3105–3114.
Chera, S., Ghila, L., Wenger, Y., Galliot, B., 2011. Injury-induced activation of the MAPK/CREB pathway triggers apoptosis-induced compensatory proliferation in hydra head regeneration. Dev. Growth Differ. 53 (2), 186–201.
Chera, S., Chera, S., Ghila, L., Dobretz, K., Wenger, Y., Bauer, C., Buzgariu, W., Martinou, J.C., Galliot, B., 2009. Apoptotic cells provide an unexpected source of Wnt3 signaling to drive hydra head regeneration. Dev. Cell 17, 279–289.
Christiaen, L., Wagner, E., Shi, W., Levine, M., 2009. Whole-mount in situ hybridization on sea squirt (*Ciona intestinalis*) embryos. Cold Spring Harb. Protoc. 2009 (12).
Cloney, R.A., 1982. Ascidian larvae and the events of metamorphosis. Am. Zool. 22, 817–826.
Davidson, B., Swalla, B.J., 2002. A molecular analysis of ascidian metamorphosis reveals

activation of an innate immune response. Development 129, 4739–4751.
Degnan, B.M., Souter, D., Degnan, S.M., Long, S.C., 1997. Induction of metamorphosis with potassium ions requires development of competence and an anterior signaling center in the ascidian *Herdmania momus*. Dev. Genes Evol. 206, 370–376.
Dehal, P., Satou, Y., Campbell, R.K., Chapman, J., Degnan, B., De Tomaso, A., Davidson, B., Di Gregorio, A., Gelpke, M., Goodstein, D.M., et al., 2002. The draft genome of *Ciona intestinalis*: insights into chordate and vertebrate origins. Science 298, 2157–2167.
Domsch, K., Papagiannouli, F., Lohmann, I., 2015. The HOX-apoptosis regulatory interplay in development and disease. Curr. Top. Dev. Biol. 114, 121–158.
Gude, D.R., Alvarez, S.E., Paugh, S.W., Mitra, P., Yu, J., Griffiths, R., Barbour, S.E., Milstien, S., Spiegel, S., 2008. Apoptosis induces expression of sphingosine kinase 1 to release sphingosine-1-phosphate as a "come-and-get-me" signal. FASEB J. 22 (8), 2629–2638.
Hernández-Martínez, R., Castro-Obregón, S., Covarrubias, 2009. Progressive interdigital cell death: regulation by the antagonistic interaction between fibroblast growth factor 8 and retinoic acid. Development 136 (21), 3669–3678.
Hueber, S.D., Lohmann, I., 2008. Shaping segments: Hox gene function in the genomic age. Bioessays 30 (10), 965–979.
Huh, J.R., Guo, M., Hay, B.A., 2004. Compensatory proliferation induced by cell death in the Drosophila wing disc requires activity of the apical cell death caspase Dronc in a nonapoptotic role. Curr. Biol. 14 (14), 1262–1266, (27).
Ikuta, T., Satoh, N., Saiga, H., 2010. Limited functions of Hox genes in the larval development of the ascidian Ciona intestinalis. Dev. May 137 (9), 1505–1513.
Ikuta, T., Yoshida, N., Satoh, N., Saiga, H., 2004. Ciona intestinalis Hox gene cluster: its dispersed structure and residual colinear expression in development. Proc. Natl. Acad. Sci. USA 101 (42), 15118–15123, (Oct 19).
Jackson, D., Leys, S.P., Hinman, V.F., Woods, R., Lavin, M.F., Degnan, B.M., 2002. Ecological regulation of development: induction of marine invertebrate metamorphosis. Int. J. Dev. Biol. 46, 679–686.
Jackson, G.A., Strathmann, R.R., 1981. Larval mortality from offshore mixing as a link beween precompetent and competent period of development. Am. Nat. 118, 16–25.
Jeffery, W.R., 2002. Programmed cell death in the ascidian embryo: modulation by FoxA5 and Manx and roles in the evolution of larval development. Mech. Dev. 118, 111–124.
Karaiskou, A., Swalla, B.J., Sasakura, Y., Chambon, J.P., 2015. Metamorphosis in solitary ascidians. Genes. Jan. 53 (1), 34–47.
Kawai, N., Ogura, Y., Ikuta, T., Saiga, H., Hamada, M., Sakuma, T., Yamamoto, T., Satoh, N., Sasakura, Y., 2015. Hox10-regulated endodermal cell migration is essential for development of the ascidian intestine. Dev. Biol. 403 (1), 43–56, (Jul 1).
Klöditz, K., Chen, Y.Z., Xue, D., Fadeel, B., 2017. Programmed cell clearance: from nematodes to humans. Biochem. Biophys. Res. Commun. 482 (3), 491–497, (Jan 15).
Knosp, W.M., Scott, V., Bächinger, H.P., Stadler, H.S., 2004. HOXA13 regulates the expression of bone morphogenetic proteins 2 and 7 to control distal limb morphogenesis. Dev. Sep 131 (18), 4581–4592.
Koussoulakos, S., 2004. Vertebrate limb development: from Harrison's limb disk transplantations to targeted disruption of Hox genes. Anat. Embryol. 209 (2), 93–105.
Lauber, K., Bohn, E., Kröber, S.M., Xiao, Y.J., Blumenthal, S.G., Lindemann, R.K., Marini, P., Wiedig, C., Zobywalski, A., Baksh, S., Xu, Y., Autenrieth, I.B., Schulze-Osthoff, K., Belka, C., Stuhler, G., Wesselborg, S., 2003. Apoptotic cells induce migration of phagocytes via caspase-3-mediated release of a lipid attraction signal. Cell 113 (6), 717–730, (13).
Li, F., Huang, Q., Chen, J., Peng, Y., Roop, D.R., Bedford, J.S., Li, C.Y., 2010. Apoptotic cells activate the "phoenix rising" pathway to promote wound healing and tissue regeneration. Sci. Signal. 3 (110), ra13, (23).
Lockshin, R.A., Williams, C.M., 1965. Programmed cell-death-I Cytology of degeneration in the intersegmental muscles of the Pernyl Silkmoth. J. Insect Phys. 11, 123–133.
Lohmann, I., McGinnis, N., Bodmer, M., McGinnis, W., 2002. The Drosophila Hox gene deformed sculpts head morphology via direct regulation of the apoptosis activator reaper. Cell 110 (4), 457–466, (Aug 23).
Mallo, M., Wellik, D.M., Deschamps, J., 2010. Hox genes and regional patterning of the vertebrate body plan. Dev. Biol. 344 (1), 7–15, (Aug 1).
Matsunobu, S., Sasakura, Y., 2015. Time course for tail regression during metamorphosis of the ascidian Ciona intestinalis. Dev. Biol. 405 (1), 71–81, (Sep 1).
Meier, P., Finch, A., Evan, G., 2000. Apoptosis in development. Nature 407, 769–801.
Monier, B., Gettings, M., Gay, G., Mangeat, T., Schott, S., Guarner, A., Suzanne, M., 2015. Apico-basal forces exerted by apoptotic cells drive epithelium folding. Nature 518 (7538), 245–248, (12).
Nakayama-Ishimura, A., Chambon, J.P., Horie, T., Satoh, N., Sasakura, Y., 2009. Delineating metamorphic pathways in the ascidian Ciona intestinalis. Dev. Biol. 326, 357–367.
Ohsawa, S., Hamada, S., Kuida, K., Yoshida, H., Igaki, T., Miura, M., 2010. Maturation of the olfactory sensory neurons by Apaf-1/caspase-9-mediated caspase activity. Proc. Natl. Acad. Sci. USA 107 (30), 13366–13371, (27).
Pasini, A., Amiel, A., Rothbacher, U., Roure, A., Lemaire, P., Darras, S., 2012. Formation of the ascidian epidermal sensory neurons: insights into the origin of the chordate peripheral nervous system. PLoS Biol. 4, e225.3.
Sasakura, Y., Kanda, M., Ikeda, T., Horie, T., Kawai, N., Ogura, Y., Yoshida, R., Hozumi, A., Satoh, N., Fujiwara, S., 2002. Retinoic acid-driven Hox1 is required in the epidermis for forming the otic/atrial placodes during ascidian metamorphosis. Development 139, 2156–2160.
Satoh, N., 1994. In: Barlow, P.W., Bray, D., Green, P.B., Slack, J.M.W. (Eds.), Developmental Biology of Ascidians. Cambridge University Press, Cambridge, 234.
Seipp, S., Schmich, J., Leitz, T., 2001. Apoptosis–a death-inducing mechanism tightly linked with morphogenesis in Hydractina echinata (Cnidaria, Hydrozoa). Development 128, 4891–4898.
Shirae-Kurabayashi, M., Nishikata, T., Takamura, K., Tanaka, K.J., Nakamoto, C., Nakamura, A., 2006. Dynamic redistribution of vasa homolog and exclusion of somatic cell determinants during germ cell specification in Ciona intestinalis. Development 133, 2683–2693.
Spagnuolo, A., Ristoratore, F., Di Gregorio, A., Aniello, F., Branno, M., Di Lauro, R., 2003. Unusual number and genomic organization of Hox genes in the tunicate Ciona intestinalis. Gene 309 (2), 71–79, (8).
Suzanne, M., Steller, H., 2013. Shaping organisms with apoptosis. Cell Death Differ. 20 (5), 669–675.
Takada, N., Yamaguchi, H., Shida, K., Terajima, D., Satou, Y., Kasuya, A., Satoh, N., Satake, M., Wang, H.G., 2005. The cell death machinery controlled by Bax and Bcl-XL is evolutionarily conserved in Ciona intestinalis. Apoptosis 10, 1211–1220.
Takamura, K., Fujimura, M., Yamaguchi, Y., 2002. Primordial germ cells originate from the endodermal strand cell in the ascidian *Ciona intestinalis*. Dev. Genes Evol. 212, 11–18.
Tarallo, R., Sordino, P., 2004. Time course of programmed cell death in Ciona intestinalis in relation to mitoticactivity and MAPK signaling. Dev. Dyn. 230, 251–262.
Tata, J.R., 1966. Requirement for RNA and protein synthesis for induced regression of the tadpole tail in organ culture. Dev. Biol. 13, 77–94.
Terajima, D., Shida, K., Takada, N., Kasuya, A., Rokhsar, D., Satoh, N., Satake, M., Wang, H.G., 2003. Identification of candidate genes encoding the core components of the cell death machinery in the Ciona intestinalis genome. Cell Death Differ. 10, 749–753.
Toyama, Y., Peralta, X.G., Wells, A.R., Kiehart, D.P., Edwards, G.S., 2008. Apoptotic force and tissue dynamics during Drosophila embryogenesis. Science 321, 1683–1686.
Tseng, A.S., Adams, D.S., Qiu, D., Koustubhan, P., Levin, M., 2007. Apoptosis is required during early stages of tail regeneration in Xenopus laevis. Dev. Biol. 301, 62–69.
Vaculova, A.1, Zhivotovsky, B., 2008. Caspases: determination of their activities in apoptotic cells. Methods Enzymol. 442, 157–181.
Vritz, S., Reiter, S., Galliot, B., 2014. Cell death: a program to regenerate. Curr. Top. Dev. Biol. 108, 12–151.
Weill, M., Philips, A., Chourrout, D., Fort, P., 2005. The caspase family in urochordates: distinct evolutionary fates in ascidians and larvaceans. Biol. Cell 97, 857–866.
Yamaguchi, Y., Miura, M., 2013. How to form and close the brain: insight into the mechanism of cranial neural tube closure in mammals. Cell. Mol. Life Sci. 70 (17), 3171–3186.